Langmuir

Article

pubs.acs.org/Langmuir

Dynamic Properties of Bicellar Lipid Mixtures Observed by Rheometry and Quadrupole Echo Decay

Alanna Flynn, Michael Ducey, Anand Yethiraj,* and Michael R. Morrow*

Department of Physics and Physical Oceanography, Memorial University of Newfoundland, St. John's, Newfoundland and Labrador, Canada, A1B 3X7

ABSTRACT: In bicellar dispersions of 1,2-dimyristoyl-*sn*-glycero-3-phosphocholine (DMPC) and 1,2-dihexanoyl-*sn*-glycero-3-phosphocholine (DHPC), the transition from isotropic reorientation to partial orientational order, on warming, is known to coincide with a sharp increase in viscosity. In this work, cone-and-plate rheometry, ^{2}H NMR spectroscopy, and quadrupole echo decay observations have been used to obtain new insights into the dynamics of phases observed in bicellar DMPC/DHPC mixtures. Samples with 25% of the DMPC component deuterated were used to correlate rheological measurements with phase behavior observed by ^{2}H NMR spectroscopy. Mixtures containing only normal DMPC (DMPC/DHPC) or only chain perdeuterated DMPC (DMPC-d_{54}/DHPC) were used to refine rheology and quadrupole echo decay measurements respectively. The viscosity peaked at 4−9 Pa·s, just above the isotropic-to-nematic transition, and then dropped as samples were warmed through the nematic-to-lamellar transition. Quadrupole echo decay times above the nematic-to-lamellar transition were significantly longer than typically observed in the liquid crystalline phase of saturated lipid multilamellar vesicles. This may indicate a damping of slow bilayer undulations resulting from the coupling of opposite bilayer surfaces by DHPC-lined pores.

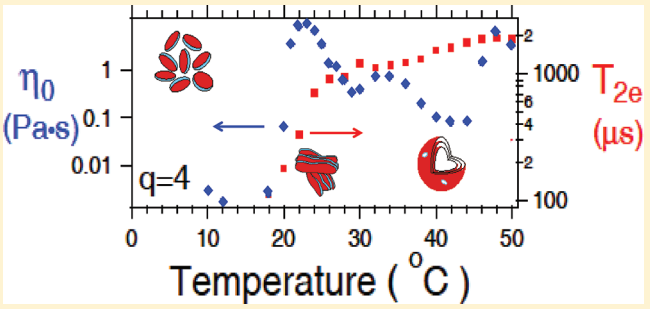

INTRODUCTION

Dispersions of short-chain and long-chain phospholipid mixtures that can assemble into magnetically orientable bilayered micelle particles[1] have been of considerable interest as platforms for solid-state NMR studies of membrane associated proteins.[2−8] Such so-called bicellar mixtures[9] are also of intrinsic importance as model lipid assemblies in which chain-length mismatch influences morphology and the distribution of lipid components between planar or highly curved environments. The phase behavior and physical properties of the particular bicellar mixture comprising 1,2-dimyristoyl-*sn*-glycero-3-phosphocholine (DMPC) and 1,2-dihexanoyl-*sn*-glycero-3-phosphocholine (DHPC) have been extensively studied using many techniques including ^{31}P and ^{2}H NMR,[1,10−13] pulsed field gradient NMR,[14−16] small angle neutron scattering,[9,17−20] small-angle X-ray scattering,[16] differential scanning calorimetry (DSC),[16,18,21,22] molecular dynamics,[23] fluorescence probe spectroscopy,[24] cryogenic transmission electron microscopy (cryo-TEM),[21,25] and capillary viscometry.[10,26]

Mixtures of DMPC and DHPC can be characterizd by the molar ratio q = [DMPC]/[DHPC]. For small values of q and/or for temperatures below the DMPC main transition, DMPC/DHPC dispersions form isotropically reorienting bilayered disk micelles, or bicelles, with the shorter chain DHPC predominantly located on the highly curved disk edges and the longer chain DMPC predominantly located in the more planar bilayer regions.[27−30] At higher q ratios (above ∼2), DMPC/DHPC dispersions transform to a magnetically orientable phase as temperature is raised through the liquid crystal to gel transition temperature of DMPC. Insights into the morphology of this phase have been provided by pulsed field gradient NMR,[14] small angle neutron scattering,[9,17,20,31−33] fluorescence probe spectroscopy,[24] and cryo-TEM[21,25] observations. NMR and fluorescence observations showed that, above the DMPC main transition temperature, bicelle disks coalesce into extended structures,[14,24] presumably with DHPC still preferentially located along the highly curved pore or micelle edges. There is now general acceptance that this magnetically orientable phase, identified by Katsaras and co-workers as a chiral nematic phase, comprises worm-like or thread-like micelles.[9,20] This phase is also distinguished by its elevated viscosity.[9,10,20,25,26] This elevated viscosity is not unexpected for wormlike micelles above the overlap concentration. The temperature range over which this phase persists is sensitive to mixture composition.[9] As temperature is raised further, the mixture transforms gradually into what appears to be a perforated lamellar phase.[9,19,20,25,34] NMR observations also indicate some migration of DHPC into more ordered planar environments[12,22] and a growing presence of small, rapidly tumbling particles[11,12,22] at higher temperatures. If the long chain component of the dispersion is a mixture of DMPC and the anionic lipid, 1,2-dimyristoyl-*sn*-glycero-3-phosphoglycerol (DMPG), the isotropically reorienting bicelle phase is reported

Received: October 20, 2011
Revised: December 23, 2011
Published: December 24, 2011

   dx.doi.org/10.1021/la204111z | *Langmuir* 2012, 28, 2782−2790

to transform directly to a perforated lamellar phase at the DMPC main transition temperature.[31,35] Further insights into morphologies of bicellar material phases have been obtained by studying diffusion of bicellar constituents[14,15,29,30] or the diffusion of other molecules through these structures.[14,36]

The DMPC/DHPC system displays a complex phase behavior and despite extensive study, as outlined above, interesting aspects of bicellar mixture behavior continue to emerge. The work reported here examines two aspects of bicellar material dynamic properties. The high viscosity of the magnetically alignable phase of DMPC/DHPC dispersion provided important clues to the morphology of this phase.[9,20,25] To our knowledge, however, direct measurements of rheological properties in this system have only been performed using capillary viscometry.[10,26] In the current work, a cone-and-plate rheometer has been used, in both steady flow and oscillating shear modes, to obtain a more detailed picture of how the shear-rate dependent viscosity of the bicellar material changes with temperature through the observed phase changes. We have also used quadrupole echo decay-time measurements on chain-deuterated DMPC (DMPC-d_{54}) in DMPC/DHPC mixtures to illustrate a significant distinction between slow motions in the bicellar material lamellar phase and in the liquid crystalline phase of more conventional lipid bilayer vesicles. In the course of this work, ^{2}H NMR spectra of DMPC/DHPC mixtures containing mixtures of normal DMPC and DMPC-d_{54} were used to connect rheology and quadrupole echo decay measurements to specific phases of the DMPC/DHPC mixtures.

MATERIALS AND EXPERIMENTAL METHODS

Bicellar lipid mixtures were prepared with DMPC/DHPC molar ratios of q = 3, q = 4, or q = 5. Depending on the measurements to be performed, the DMPC content of a given sample was 100% normal DMPC, 100% DMPC-d_{54}, or a 3:1 mixture of DMPC and DMPC-d_{54}. For a given sample, the appropriate mixture of dry lipids was dissolved in 2:1 (v/v) chloroform/methanol. Solvent was removed by rotary evaporation at 45 °C followed by 8−10 h of being held under vacuum in a desiccation chamber. Samples were then hydrated by gentle washing in an appropriate volume of 100 mM HEPES buffer (pH 7) followed by vortexing and a 15 min period of immersion in a sonicating bath with no heat applied. Samples were then subjected to 5 cycles of freezing in liquid nitrogen and thawing at 40 °C to facilitate mixing and disruption of residual multilamellar vesicles. After preparation, samples were held at approximately −8 °C prior to use.

The presence of salts has been demonstrated to enhance magnetic orientability of bicellar samples.[37] The phase diagrams reported by Harroun and co-workers, however, were obtained from samples prepared without added salt or buffer. For the current work, extra salts were not added to samples. The decision to prepare samples in this way reflected a concern that any possible sensitivity of particle morphology to salt concentraton might complicate the consistent preparation of samples for rheology and NMR and introduce additional uncertainty into the comparison of results from the two approaches.

The lipid weight fraction in all samples was roughly 0.1. Samples intended for rheometry studies alone were prepared using DHPC and normal DMPC with a total dry lipid mass of 100 mg and were hydrated in 1 mL of buffer. Samples intended for parallel ^{2}H NMR and rheometry studies were prepared using DHPC and a 3:1 mixture of DMPC and DMPC-d_{54}. The total dry lipid mass was again 100 mg and samples were hydrated in 1 mL of buffer. After the hydration, sonication, and freeze−thaw cycling steps, ∼ 250 μL of the dispersion was transferred to an 8-mm diameter NMR tube with the remainder being used for rheometry. Samples intended for ^{2}H NMR only were prepared using DMPC-d_{54} and a total dry lipid mass of 25 mg. These samples were hydrated in 250 μL of buffer following the protocol described above and the entire sample was then transferred to an 8-mm diameter NMR tube. All lipids were purchased from Avanti Polar Lipids (Alabaster, Ala) and used without further purification. A multilamellar vesicle sample of DMPC-d_{54} was prepared by similarly dissolving, hydrating, and drying the lipid film but without the sonication and freeze−thaw steps used to prepare the bicellar mixture samples.

^{2}H NMR. Deuterium NMR spectra were obtained using either a 3.5 or 9.4 T superconducting magnet in conjunction with a locally built spectrometer. Spectra were acquired using a quadrupole echo sequence.[38] The $\pi/2$ pulses were 2.2−4.5 μs long. The separation between $\pi/2$ pulses in the quadrupole echo sequence was 35 μs. Oversampling[39] was used to obtain effective dwell times of 4 μs. For samples with 25% DMPC deuteration, between 4,000 and 8,000 transients were averaged to obtain free induction decays that were then Fourier transformed to spectra. For samples with fully deuterated DMPC, 1200 transients were averaged. For echo decay measurements, the number of transients averaged ranged from 400 to 4000 depending on the sample size and the extent to which DMPC was deuterated.

For deuterons attached to bonds undergoing fast, axially symmetric reorientation about the bilayer normal, the orientational order parameter is

$$S_{CD} = \frac{1}{2}\langle 3\cos^2 \theta_{CD} - 1\rangle \quad (1)$$

where θ_{CD} is the angle between the carbon-deuterium bond and the symmetry axis for molecular reorientation. The average is over accessible chain conformations.

For samples in which the bilayer normal is preferentially oriented perpendicular to the magnetic field, the spectrum of a chain-perdeuterated lipid like DMPC-d_{54} undergoing fast, axially symmetric reorientation is a superposition of doublets with each deuteron contributing at a splitting

$$\Delta\nu = \frac{3}{4}\frac{e^2qQ}{h}S_{CD} \quad (2)$$

where $(e^2qQ)/h$ = 167 kHz is the quadrupole coupling constant for carbon-deuterium bonds.[40] In fluid bilayer phases, chain orientational order is highest near the headgroup end of the chain, where motion is most constrained, and decreases with position toward the methyl end of the chain. This dependence of orientational order on position along the acyl chain can be represented graphically as an orientational order parameter profile.[40−42] Orientational order typically decreases only slowly with position near the headgroup end of the chain. The resulting plateau in the order parameter profile results in a concentration of intensity at the splitting corresponding to the most ordered portion of the chain. In the nematic bicellar phase, the extent to which intensity is concentrated at the quadrupole splittings for each position along the acyl chain is indicative of the degree of magnetic orientation. Concentration of intensity near the plateau splitting is particularly prominent for oriented bilayers.

For samples in which bilayer normal orientation is spherically distributed, such as dispersions of multilamellar vesicles, the resulting spectrum is a superposition of Pake doublets. The result is a flatter distribution of intensity between prominent edges having the same distribution of splittings as would be seen for an oriented sample of such bilayers. For samples consisting of isotropically reorienting bilayer particles, such as the low temperature bicelle phase, the spectrum collapses to a narrow line.

The dependence of quadrupole echo amplitude on the time, 2τ, between the first $\pi/2$ pulse in the quadrupole echo pulse sequence and the refocusing of the echo, was obtained by collecting echos for pulse separations varying between τ = 35 and 200 μs.

Microscopy. Cross-polarizer optical microscopy was carried out as a function of temperature using a Nikon Eclipse 80-i upright microscope equipped with a manually crossable polarizer and an analyzer. The microscopy sample was prepared between No. 1 coverslips, with strips of No. 0 coverslips as 100 μm spacers, and sealed

dx.doi.org/10.1021/la204111z | Langmuir 2012, 28, 2782−2790

using Norland epoxy NOA 68 and cured under a UV lamp. It was then placed on an aluminum plate with a circular window and inside an Instek HCS 61 hot stage at 10 °C. The temperature was increased in a 0.1 °C/min ramp and images were acquired once per minute with a 12-bit monochrome camera (Qimaging QICAM Fast 1394).

Rheometry. Rheological measurements on normal (nondeuterated) and partially deuterated lipid samples were carried out using an Anton Paar MCR 301 rheometer. A 50 mm diameter cone-and-plate rheometer tool (cone angle 1°) was filled with approximately 0.5 mL of the mixed lipid sample, with the temperature set by a temperature-controlled plate and enclosure to reduce thermal gradients. The enclosure had rubber air seals that minimized evaporation. For each viscosity measurement, three flow curves (stress versus strain rate) were obtained and the results averaged after ascertaining that the results from the 3 measurements were consistent. The flow curves reported here are these averaged results. The oscillatory shear measurements (storage and loss modulus versus angular frequency) reported here were carried out prior to the third flow curve measurement.

Flow curves were obtained between shear rates $\dot{\gamma}$ = 0.1 and 500 s^{-1}. In this study, only the small and intermediate shear rates $\dot{\gamma}$ < 300 s^{-1} were analyzed.

Oscillation measurements were carried out strain amplitude of 0.05 (in the linear viscoelastic regime) and up to angular frequency ω = 500 s^{-1}. The storage (G') and loss (G'') moduli were obtained as a function of ω, from which the complex viscosity amplitude $|\eta^*| = [(G''/\omega)^2 + (G'/\omega)^2]^{0.5}$ was obtained.

RESULTS AND DISCUSSION

^{2}H NMR Spectroscopy. Figure 1 shows ^{2}H NMR spectra for DMPC-d_{54}/DMPC/DHPC samples with molar DMPC (total) to DHPC ratios of q = 3, q = 4, and q = 5. For each sample, the spectra at low temperature reflect isotropic reorientation of small particles, presumably bicelle disks, on a time scale much shorter than the ~10^{-5} s characteristic time for the ^{2}H NMR experiment. At 24 °C for q = 3, 19 °C for q = 4, and 20 °C for q = 5, a broad spectral component spanning about ±12 kHz appears. This is close to the quadrupole splitting expected for deuterons on motionally constrained chain segments near the lipid headgroup in a bilayer phase. The emergence of this spectral component reflects the onset of anisotropic reorientation about the bilayer normal. The absence of sharp doublet edges indicates that the correlation time for lipid reorientation is too long for the motion to be axially symmetric on the quadrupole echo time scale. The transition from isotropic to anisotropic reorientation presumably corresponds to aggregation of bicelle disks into the worm-like micelle phase that has been identified as a chiral nematic phase.[20]

At T = 32 °C, the q = 3 spectrum sharpens into partially resolved doublets with a concentration of doublet intensity at the splitting corresponding to the lipid chain orientational order parameter plateau. This spectrum is characteristic of fast axially symmetric lipid reorientation about a symmetry axis that is preferentially oriented perpendicular to the magnetic field and thus indicates magnetic orientation of the bicellar nematic phase. Figure 1d shows that on warming from 32 to 34 °C, the distribution of intensity between the prominent edges of the q = 3 spectrum becomes much flatter. This change to a more spherical distribution of bilayer normal orientations is indicative of the nematic to lamellar transition. For q = 4 and 5, intensities in the spectra at 28 and 30 °C are not as concentrated at splittings corresponding to perpendicular bilayer normal orientation. While these spectra indicate only slight orientation of the q = 4 and 5 samples in the 3.5 T magnetic field, the

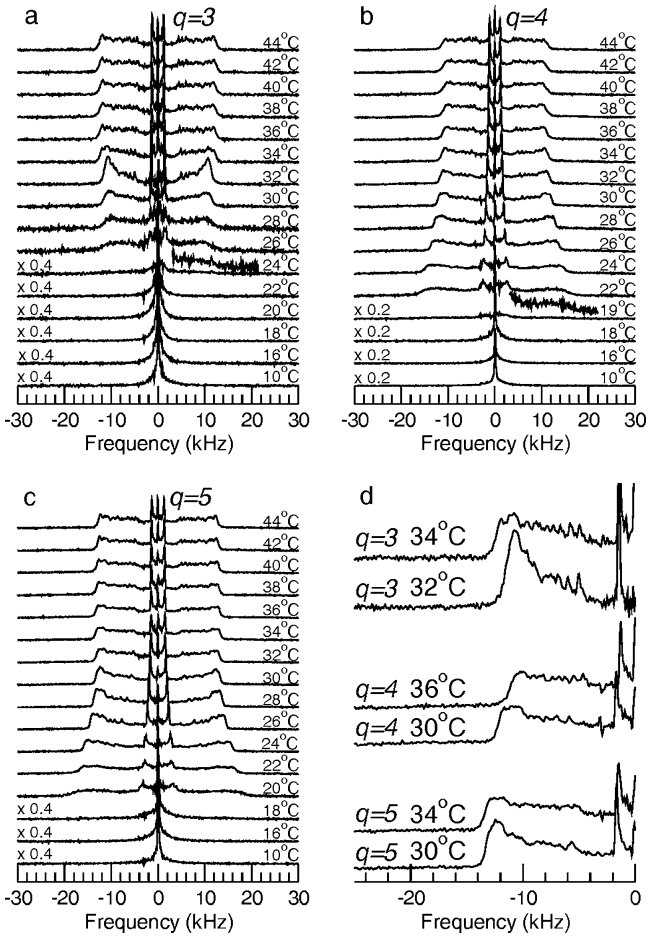

Figure 1. ^{2}H NMR spectra of DMPC-d_{54}/DMPC/DHPC mixtures. In each sample, the DMPC-d_{54}/DMPC ratio is 1:3 and the ratios of total DMPC to DHPC are (a) q = 3, (b) q = 4, and (c) q = 5. In panels a and b, portions of the spectra at 24 and 19 °C, respectively, are scaled to ×1.2 and overlaid to show the emergence of intensity near ±12 kHz. Panel d compares spectral detail near the prominent edge region corresponding to the plateau in the orientational order parameter profile at temperatures presumed to fall in the nematic and lamellar ranges of each sample. Spectra were obtained in a field of 3.5 T.

distribution of intensity between prominent spectral edges does flatten with increasing temperature beyond this range suggesting that these samples still undergo a transition from a partially ordered phase to an unoriented lamellar phase. For q = 5, this flattening is most apparent between 30 and 32 °C. For q = 4, the change is more gradual. Incomplete orientation of DMPC/DHPC mixtures in the intermediate temperature phase was seen previously under some conditions and may reflect the small magnetic field used for these spectra.[22] The sequence of spectra in Figure 1, particularly for q = 3, is generally consistent with these mixtures undergoing a sharp transition from bicelle disks to worm-like micelles, on warming through the DMPC gel-to-liquid crystal transition temperature, and then undergoing a more gradual change to a lamellar phase at higher temperature. In order to gain further insight into the properties of the mixtures in these phases, microscopic observations and rheological measurements were carried out on corresponding samples made with normal lipids and on fractions of each DMPC-d_{54}-doped sample. As noted below, comparison of viscosity observations for the three DMPC-d_{54}/DMPC/DHPC samples from which the spectra in Figure 1 were obtained

dx.doi.org/10.1021/la204111z | Langmuir 2012, 28, 2782−2790

suggest that, despite differences in apparent magnetic orientability, as evidenced by the relative enhancement of intensity at the prominent edges of the spectra, these samples did undergo similar rheological changes with increasing temperature.

Microscopy. Polarized-light optical microscopy was carried out on the partially deuterated $q = 3$ sample used for deuterium NMR. The transition from isotropic to nematic was nearly unobservable. This is in contrast to previous work in which the nematic phase displayed a characteristic "fingerprint" pattern.[9] Untreated glass induces roughly homeotropic alignment, but with a substantial degree of variability in alignment orientation. Thus unobservability, while not conclusive, strongly indicates weak nematic ordering. What is extremely clear however is that at approximately 39 °C (Figure 2), there is a very pronounced

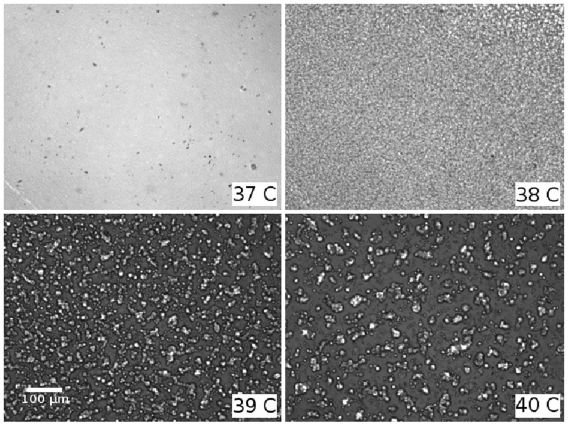

Figure 2. Crossed-polarizer optical micrographs near a phase transition for $q = 3$.

transition from homogeneity to heterogeneity on the μm length scale. This is roughly coincident with the change in the temperature dependence of the low-shear-rate viscosity with a minimum at approximately 39 °C (shown in Figure 7 below). The change in sample appearance at this transition is consistent with previously reported observations of dilute bicellar samples by polarized optical microscopy.[9,20]

Rheology. Previous viscosity measurements carried out on the DMPC/DHPC system suggest the potential usefulness of rheology for identifying phase transitions.[10,26] A detailed study of rheology as a function of temperature was carried out for samples with three DMPC/DHPC ratios. In order to correlate with ^{2}H NMR observations, rheology studies were also conducted, in parallel with the NMR studies illustrated in Figure 1, on the samples prepared with a 3:1 mixture of DMPC and DMPC-d_{54}. Observed viscosities were not found to be significantly affected by partial deuteration for any of the DMPC/DHPC ratios studied, apart from a 1.3 °C shift. This is illustrated by the comparison of results for the normal and partially deuterated $q = 5$ samples shown in Figure 4 below, where the results for the deuterated sample have been shifted to the right by 1.3 °C.

Steady Shear. Measurements of shear stress σ versus strain rate $\dot{\gamma}$ were used to generate flow curves in the $\dot{\gamma} = 0.1-300$ s^{-1} range. Figure 3 shows the dependence of $\eta(\dot{\gamma}) = \sigma/\dot{\gamma}$ on $\dot{\gamma}$ for different temperatures in the $q = 5$ sample. At temperatures below 20 °C, the flow curves are linear and $\eta(\dot{\gamma})$ is constant. This behavior can be immediately identified as characteristic of the isotropic phase. At temperatures above 20 °C, shear-

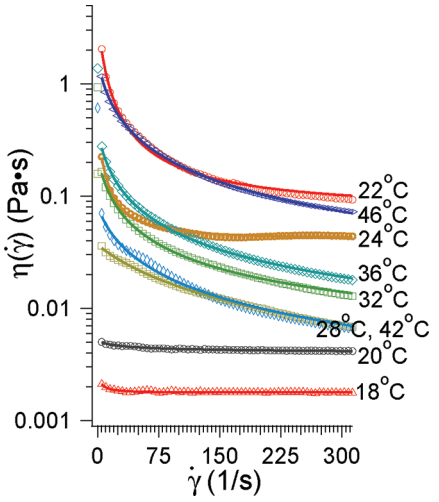

Figure 3. $\eta(\dot{\gamma}) = \sigma/\dot{\gamma}$ versus shear rate at different temperatures ($q = 5$). The character of the flow curves (σ vs $\dot{\gamma}$) changes from linear (Newtonian) for temperatures below 20 °C ($\eta(\dot{\gamma})$ is constant) to shear-thinning at higher temperatures (decreasing $\eta(\dot{\gamma})$) for intermediate shear rates.

thinning behavior was observed. The low-shear-rate $\eta(\dot{\gamma})$ was extrapolated to zero to yield the zero-shear-rate viscosity η_0. The physically reasonable Cross equation

$$\eta - \eta_\infty = (\eta_0 - \eta_\infty)/(1 + (\tau\dot{\gamma})^n) \quad (3)$$

is a crossover function connecting low-shear-rate viscosity to high-shear-rate limiting viscosity[43] and describes shear-thinning behavior in a number of systems, including wormlike micellar phases.[44] We fit our results to the Cross equation constraining the zero-shear-rate viscosity to within 5 standard deviations of the linear fitted value. This gave reasonably good fits for most sample temperatures.

In lyotropic lamellar phases, shear thinning has been described by a simple power law $\sigma \approx \dot{\gamma}^x$. The reported values of the exponent vary. Roux et al.[45] find $x = 0.2$, whereas Meyer et al.[46] and Lu et al.[47] find $x = 0.6$ and 0.7, respectively, in the shear-thinning regime. It should be noted that at no temperature is the shear thinning behavior describable by the simple power law observed in lyotropic lamellar systems referred to above.[45−47] From the above analysis we obtain the temperature dependences of η_0 (Figure 4) and η_∞ (Figure 5).

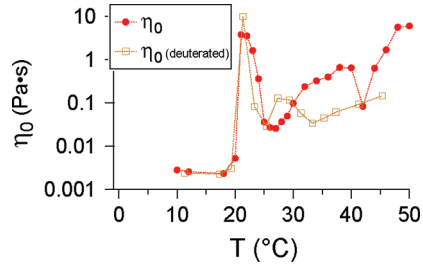

Figure 4. Zero-shear-rate viscosity as a function of temperature for $q = 5$. Results for the sample containing 3:1 DMPC/DMPC-d_{54} (triangle) show a similar trend, but with the isotropic-worm-like micelle transition shifted to lower temperature by 1.3 °C.

The fit to eq 3 also yields a characteristic time scale τ (also shown in Figure 5) and a power law exponent n which is found to be 1.1 ± 0.2. It is noted that only one viscosity (η_0) is

dx.doi.org/10.1021/la204111z | Langmuir 2012, 28, 2782−2790

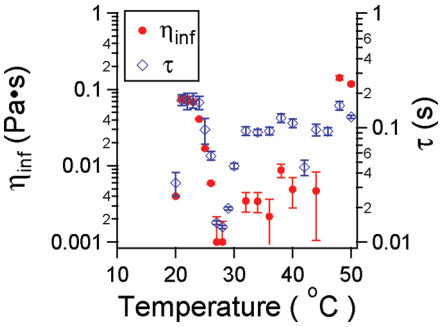

Figure 5. Characteristic time scale τ and high-shear viscosity η_{inf} versus temperature in the q = 5 sample based on the crossover from linear to shear-thinning regimes (from fit to Cross model, see text).

observed in the isotropic phase and neither n nor τ is meaningful here. However τ is a meaningful time scale at higher temperatures where it varies from 2 to 100 ms. It represents a characteristic shear-thinning time scale. All of the quantities obtained exhibit clear changes in behavior at consistent temperature values, and it should therefore be reasonable to extract meaningful information about phase behavior from these results.

These observations can be contrasted with the flow curves and temperature dependence of viscosity observed for a dispersion of pure DMPC multilamellar vesicles, shown in Figure 6. Here we see that $\eta(\dot{\gamma})$ is practically independent of

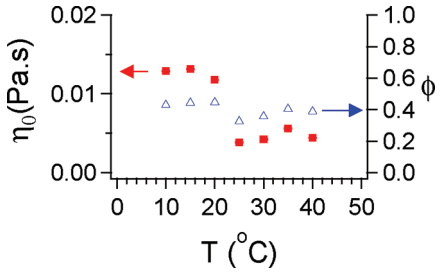

Figure 6. There is a linear relationship between stress and strain rate for pure DMPC over the entire range of strain rate probed. Shown is the zero-shear-rate viscosity and particle volume fraction for pure DMPC solution at temperatures between 10 and 40 °C. Both exhibit a distinct decrease between 20 and 24 °C.

shear rate at all temperatures with a zero-shear-rate viscosity that is ~0.01 Pa·s for T = 20 °C or lower and ~0.004 Pa·s for T = 24 °C or higher (Figure 6). The behavior of lipid vesicles as colloidal particles, implied by these results, is consistent with previous observations by de Haas and co-workers[48] but the drop in viscosity between 20 and 24 °C (the transition from the gel to the liquid crystal phase) runs counter to the increase observed in that study of small unilamellar vesicles.[48] The low-shear-rate viscosity in hard-sphere colloidal suspensions is known to increase with increasing particle volume fraction in a way that is well expressed by the phenomenological form $\eta_0 = \eta_{solvent}(1 - \varphi/0.63)^{-2}$ where φ is the particle volume fraction. Our results thus imply particle volume fractions of φ = 0.43–0.45 and 0.33–0.40 in the gel and the liquid crystal phase respectively. This suggests a decrease rather than an increase in the volume per vesicle upon crossing from the gel to the liquid crystal phase, contrary to the results of de Haas et al.[48] This could arise from a difference in either vesicle hydrodynamic size or vesicle deformability.

Figure 7 compares plots of low-shear-rate viscosity as a function of temperature, obtained from shear stress versus

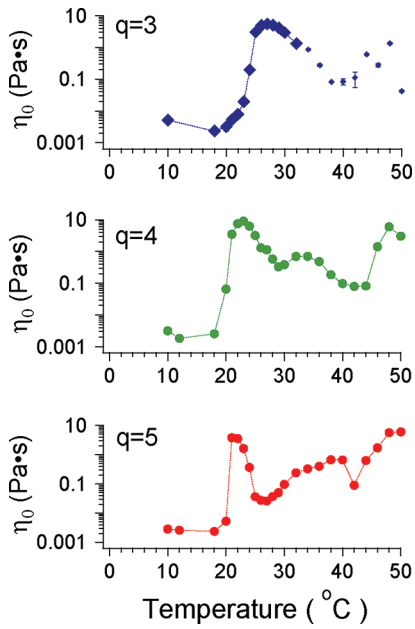

Figure 7. Low-shear-rate viscosity as a function of temperature q = 3, 4, and 5. All samples show roughly consistent rheological characteristics, with a sharp increase in viscosity at the isotropic-wormlike micellar phase (near 20 °C), followed by a gradual change at intermediate temperatures (in the 25–35 °C range) and an increase at high temperatures (close to 40 °C).

strain rate measurements, for the 3 molar ratios, q = 3, q = 4, and q = 5. The lowest plot is for q = 5 (reproduced from Figure 4 for comparison with the other molar ratios). This data shows a relatively unchanging low shear viscosity between 10 and 18 °C. This is followed by a sharp increase of the low shear viscosity at 20 °C and more gradual decrease up to 26 °C. The increase in viscosity (to 4 Pa·s at 21 °C) correlates strongly with the emergence of orientational order, as inferred from the NMR spectra, and may be identified with the coalescence of small bilayered disks into more extended structures, presumably worm-like micelles. The low-shear-rate viscosity increases steadily between 26 and 40 °C. The corresponding time scales and high-shear viscosities (shown for q = 5 in Figure 5) also show a change in behavior at ~26–28 °C. A distinct third regime of steadily increasing viscosity appears to span the 42–50 °C temperature range.

The middle plot in Figure 7 shows results for q = 4. This curve is similar to that of q = 5; clear changes in behavior occur near 20 °C, 26 °C, and again at 44 °C with nonmonotonic behavior in between and a shallow peak at ~33 °C. This is to be compared with NMR observations (Figure 1) which show the emergence of partial orientational order at 22 °C and a gradual flattening of the intensity distribution across the spectrum for temperatures above 30 °C.

The uppermost plot of Figure 7 shows the temperature dependence of low-shear-rate viscosity for q = 3. It is important to note that this plot contains two curves. The first was derived from a sample that was tested from 10 to 32 °C. Afterward, it was apparent that a broader temperature range was required to complete all phase transitions in these samples and the measurement was repeated on a new sample with the same

dx.doi.org/10.1021/la204111z | Langmuir 2012, 28, 2782–2790

molar ratio. Once again, the transition to the partially ordered phase as seen by NMR (at 26 °C) corresponds well with the rise of the low-shear-rate viscosity to 1 Pa·s. The clear increase in orientation displayed by the NMR spectrum at 32 °C is not matched by any dramatic changes in rheological behavior. There is, again, a change in rheological behavior at 40 °C, which does not correspond to any observable change in the corresponding NMR spectra.

We cannot make direct comparisons between our measurements and the viscosities measured by Struppe and Vold[10] or by Hwang et al.[26] The lipid solutions used by Hwang et al. contained 25% lipid by weight[26] and it is not clear if all viscosities measured were in the limit of low shear, as measurements appear to have been made with glass capillaries of varying sizes (and therefore different shear rates). Nevertheless it is worth mentioning that the results of Hwang et al., for q = 3.2 and 25% lipid by weight, and those of Struppe and Vold, for q = 2.9 and 10% lipid by weight, display peaks in viscosity that are somewhat higher (>10 Pa·s) than those reported here. An increase of viscosity with volume fraction would be expected especially at the onset of a worm-like micelle phase if the volume fraction crossed the threshold micellar overlap concentration.[49] This could be so in the case of Hwang et al but not in the experiments of Struppe and Vold. The reason for this discrepancy in viscosities between the latter and our work remains unclear. Regardless, the temperature ranges for the viscosity peaks in the earlier work are between 25 and 35 °C and thus largely consistent with the observations reported here.

Measurements carried out on partially deuterated mixtures (with coarser temperature resolution) showed consistent results. In the q = 5 sample, if one uses the isotropic-worm-like micelle transition as an indicator, the transition temperatures are 1.3 °C lower for the 3:1 DMPC:DMPC-d_{54} sample. Results for the nondeuterated and partially deuterated samples at q = 3 and 4 are similarly comparable.

Oscillatory Shear. Oscillatory shear measurements provided values for the storage modulus G' and the loss modulus G'' as a function of angular frequency ω. A useful way of quantifying the behavior under oscillatory shear is via the modulus of the complex viscosity $|\eta^*|$. In many soft materials one sees a phenomenological correspondence between the functional behavior of $|\eta^*|$ versus ω and that of the dynamic viscosity η versus $\dot{\gamma}$. This is termed the Cox–Merz rule[50] and is on firm footing for dilute polymer systems.[51] It has been shown that the Cox–Merz relationship is valid for dilute colloidal suspensions of hard spheres.[52] Noncompliance with the Cox–Merz rule is a useful indicator of morphology change or structural reorientation induced by large-amplitude shear.

For temperatures below 20 °C, $|\eta^*|$ is larger than η_0 for small ω (Figure 8, left), meaning that the Cox–Merz rule is not valid. The isotropic phase in our samples is, however, likely composed of disklike colloids, and it is not unreasonable to posit the alignment of these disks in the presence of large-amplitude shear, but not as a result of small-amplitude oscillatory shear. Aligned disks might indeed be expected to exhibit a lower viscosity. As temperature is increased the η_0 and $|\eta^*|$ curves converge toward each other (Figure 8, top middle and right).

Measurements in the 30–40 °C temperature range were consistent with Cox–Merz behavior (also shown in Figure 8 for q = 5). As an example, while the complex viscosities at 28 and 30 °C are very similar (both have loss tangents of around 2 at

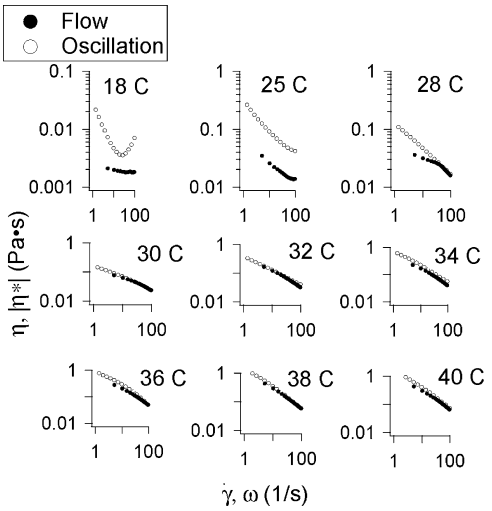

Figure 8. Steady shear viscosity η_0 ("flow") compared with complex viscosity amplitude $|\eta^*|$ ("oscillation") at low and intermediate temperatures for q = 5.

low frequencies and increasing at higher frequencies), it is the flow curves that are different.

It should be noted however that in this temperature range the viscosities are in the 0.1 Pa·s range or larger. This is in contrast with the situation at lower temperatures where the viscosities are in the 0.01 Pa·s range, and small differences between $|\eta^*|$ and η_0 are more noticeable on a logarithmic scale. Nevertheless, the correspondence between $|\eta^*|$ and η_0 in the 30–40 °C temperature range suggests that the structures probed in this regime via small-amplitude oscillatory shear and by steady shear are the same. On the other hand, in other regimes steady shear has the capability to break up structures that would not be broken up by small amplitude shear.

Quadrupole Echo Decay. By varying the interval between pulses in the quadrupole echo sequence, it is possible to measure the characteristic decay time for the quadrupole echo and gain some insight into motions that modulate the orientation-dependent quadrupole interaction for deuteron i with correlations times either longer or shorter than $(\Delta M_{2i}^j)^{-1/2}$ where ΔM_{2i}^j is the second moment of that portion of the quadrupole interaction for deuteron i modulated by a given motion j.[53] Quadrupole echo decay times in the nematic and lamellar phases of the samples with 25% of the DMPC content deuterated (not shown) were generally much longer than typically observed in the liquid crystalline phase of multilamellar vesicle (MLV) samples of chain perdeuterated disaturated phospholipids like DMPC-d_{54}. To confirm this difference, spectra and quadrupole echo decay measurements were carried out at 9.4T on DMPC-d_{54}/DHPC at q = 4 and on a multilamellar vesicle sample of DMPC-d_{54} alone. As can be seen from Figure 9, comparison of the quadrupole echo decay times for these samples do indicate a significant difference between lipid dynamics in the partially ordered phases of DMPC-d_{54}/DHPC at q = 4 and motions in the liquid crystalline phase of DMPC-d_{54} MLVs. In Figure 9b, spectra in the range 24–28 °C are also characteristic of substantially greater magnetic orientation than seen in Figure 1 for the partially deuterated q = 4 sample. The enhanced orientation may reflect the difference in magnetic fields for the two observations.

dx.doi.org/10.1021/la204111z | Langmuir 2012, 28, 2782–2790

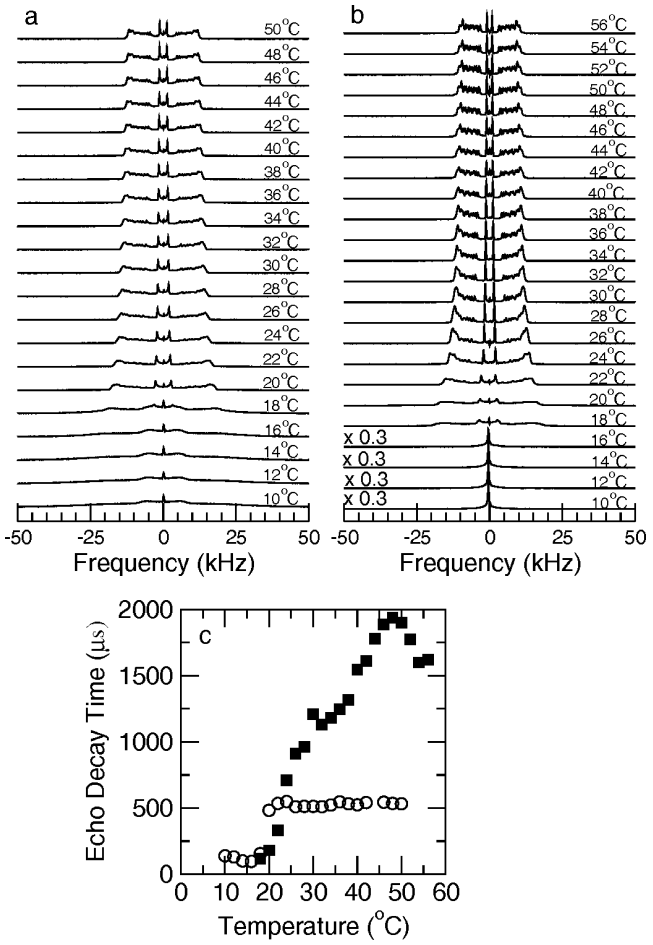

Figure 9. (a) Deuterium NMR spectra of DMPC-d_{54} multilamellar vesicles. (b) Deuterium NMR spectra of DMPC-d_{54}/DHPC mixture for q = 4. (c) Quadrupole echo decay times for (circle) DMPC-d_{54} multilamellar vesicles and for (square) DMPC-d_{54}/DHPC at q = 4. Spectra and echo decay measurements were done at 9.4 T.

For a given separation, τ, of the $\pi/2$ pulses in the quadrupole echo sequence, the echo amplitude $S(2\tau)$, at $t = 2\tau$, can be written as a sum over contributions from deuterons, labeled i, at all sites along the chain and over all orientations of the bilayer normal. The echo amplitude is thus $S(2\tau) = \Sigma_i S_i(0)e^{-R_i 2\tau}$ where R_i is the echo decay rate for a given deuteron i due to all motions that modulate the quadrupole interaction for that deuteron.[54,55] In the limit of short τ, echoes decay exponentially with a characteristic time T_2^{qe} and the average of the echo decay rate over the entire population of deuterons can be taken to be $\langle R \rangle = (T_2^{qe})^{-1}$.

For a given deuteron i, the contribution to the echo decay rate R_i^j from a slow motion j, such that $\tau_{ci}^j \gg (\Delta M_{2i}^j)^{-1/2}$, is proportional to the correlation time[53,56] so that $R_i^j \propto (\tau_{ci}^j)^{-1}$. For fast motions with $\tau_{ci}^j \ll (\Delta M_{2i}^j)^{-1/2}$, the contribution is $R_i^j = \Delta M_{2i}^j \tau_{ci}^j$. In the liquid crystalline phase of a multilamellar dispersion, the quadrupole interaction is modulated by a superposition of fast motions (such as trans−gauche isomerization, reorientation about the bilayer normal and fluctuations of the lipid long axis away from the bilayer normal) and slow motions (such as bilayer undulations). As temperature is reduced, correlation times tend to increase. The net effect of motions in the MLV liquid crystalline phase tends to be an echo decay time between 500 and 1000 μs and largely independent of temperature.[54,55] As temperature is lowered through the liquid crystal to gel transition, motions (with the exception of trans−gauche isomerization) that were fast in the liquid crystalline phase slow down and transit into the slow motion regime, as defined by comparison of the correlation time with $(\Delta M_{2i}^j)^{-1/2}$, whereas motions that were slow in the liquid crystalline phase become even slower or freeze out. The result is a minimum in echo decay time at the transition.

Figure 9 shows spectra over a range of temperatures for DMPC-d_{54} multilamellar vesicles and for a q = 4 mixture of DMPC-d_{54}/DHPC along with corresponding plots of echo decay time versus temperature. For the DMPC-d_{54} MLV sample, echo decay times are largely independent of temperature in the liquid crystalline phase. The observed echo decay time, 500 μs, is typical of multilamellar vesicle samples for disaturated phospolipids.[54,55] For the mixture of DMPC-d_{54}/DHPC at q = 4, the quadrupole interaction is averaged away in the isotropic phase and echo decay measurements start with the onset of partial ordering. For temperatures corresponding to the magnetically oriented phase, echo decay times are longer than for the multilamellar phase. For higher temperatures, echo decay times are significantly larger than 1000 μs and thus larger than typically seen in the liquid crystalline phase of MLVs. The DMPC-d_{54}/DHPC echo decay times peak at ∼48 °C and drop slightly at higher temperatures. Because contributions to echo decay rate for a given deuteron sum, the observation of a very large echo decay time implies that at least one of the contributions to the echo decay rate in the high temperature phase of the bicellar material must be much smaller than the corresponding contribution in an MLV sample. In effect, the observed difference suggest either that fast motions in the high temperature phase of the bicellar material are much faster (or of smaller amplitude) than in the liquid crystalline MLV phase or that corresponding slow motions are much slower.

Another interesting difference between DMPC-d_{54} MLVs and the high temperature phase of the DMPC-d_{54}/DHPC dispersion is the distribution of quadrupole splittings in spectra above ∼50 °C as seen in Figure 9. The sharp drop in intensity beyond the prominent edges at ∼ ± 12kHs is characteristic of a chain orientational order parameter profile with a flat plateau corresponding to a weak dependence of orientational order on methylene position near the headgroup end of the lipid acyl chain.[40−42] For the DMPC-d_{54}/DHPC dispersion, the largest splitting is not coincident with the highest density of splittings. This shape, which can be seen in higher temperature spectra shown in some earlier studies of DMPC/DHPC mixtures,[11,12] indicates that the most ordered portion of the chain does not correspond to the flattest portion of the orientational order parameter profile. This perturbation of DMPC-d_{54} orientational order at high temperature likely reflects migration of the shorter chain DHPC into more the planar DMPC-d_{54}-rich environment as temperature is raised. Increased mixing of DMPC and DHPC has been assumed to account for the increase in DHPC-d_{22} chain order at high temperature[12,22] and has recently been inferred from ^{31}P NMR observations[36] and also discussed in the context of temperature-driven annealing of perforations in bicellar lamellar phases.[57]

Because the high-temperature DMPC-d_{54}/DHPC spectra differ from the corresponding DMPC-d_{54} MLV spectra primarily in the distribution of quadrupole splittings rather than in the magnitude of those splittings, the very long quadrupole echo decay times observed for the DMPC-d_{54}/DHPC dispersion likely reflect a perturbation of slower

dx.doi.org/10.1021/la204111z | Langmuir 2012, 28, 2782−2790

motions. One possibility is that pores formed by accommodation of DHPC in the lamellar phase mechanically couple opposite sides of the bilayer and stiffen it so that slow undulations are damped. The observation that the echo decay time peaks and then drops beyond temperatures where mixing of DHPC and DMPC may be perturbing the distribution of DMPC-d_{54} quadrupole splittings in the plateau region of the orientational order parameter is consistent with this possibility.

CONCLUSIONS

The observations reported here provide a more detailed picture of the rheology of DMPC/DHPC bicellar dispersions and demonstrate some interesting distinctions between the high temperature properties of such dispersions and those of MLV dispersions under corresponding conditions. Viscosity was found to increase sharply as DMPC/DHPC dispersions were warmed through the isotropic-to-nematic transition at which small bicellar disks coalesced into more extended structures and spectra for DMPC-d_{54} indicated a change from isotropic reorientation to partial orientational order. Comparison of small-amplitude oscillatory shear and large-amplitude steady shear (flow) measurements indicated a divergence of flow and oscillation viscosities below this transition and a convergence of flow and oscillation viscosities for increasing temperatures above this transition. This was attributed to the change, for large-amplitude shear, from flow-alignable disklike particles at lower temperature to more extended structures at higher temperature, a picture that is consistent with current understanding of this transition.

Above the isotropic-to-nematic transition, ^{2}H NMR spectra of the DMPC-d_{54} component in the dispersion indicated reorientation with an increasing degree of axial symmetry and some magnetic alignment as temperature was raised. As the temperature was raised further, there was a gradual flattening of intensity across the spectrum as it became increasingly characteristic of a lamellar morphology. The temperature dependence of viscosity over this range was more complex. For all three DMPC/DHPC ratios examined, viscosity dropped to a local minimum at a temperature a few degrees above that of the viscosity peak and then to a second minimum close to 40 °C, a temperature at which one sample, q = 3, displayed visible aggregation under polarizing light microscopy.

For temperatures above ∼34 °C, the ^{2}H NMR spectra for all of the samples examined changed only gradually and, except for a perturbed distribution of splittings in the plateau region of the spectrum at high temperature, appeared to be superficially similar to those obtained from MLV dispersions of disaturated phospholipids under similar conditions. However, the magnitude and temperature dependence of viscosity, which reflect flows on millisecond to second time scales, and the large echo decay times observed in this range, which reflect motions on $\sim 10^{-7}$ -10^{-5}s time scales, demonstrate significant differences between the high temperature properties of DMPC/DHPC dispersions and those of DMPC multilamellar vesicle dispersions under corresponding conditions. While this difference in time scales makes a direct comparison between viscosity and echo decay times challenging, there are nevertheless some strong self-consistencies evident. In the q = 4 sample, the viscosity increases sharply above 20 °C while T_2^{qe} reaches an inflection point at a value near 1000 μs. At 40 °C, the slope of T_2^{qe} versus T increases and T_2^{qe} rises to a peak at ∼50 °C. The viscosity of the corresponding sample also exhibits a sharp rise between 40 and 50 °C. In the pure DMPC sample, a sharp increase in T_2^{qe} at 20 °C correlates strongly with a sharp decrease in the viscosity. Above 20 °C, for pure DMPC, both the viscosity and T_2^{qe} are roughly constant. The differences in lamellar-phase viscosity and echo decay time between DMPC and the bicellar mixtures likely reflect the overall morphology of the lamellar DMPC/DHPC structures, the presence of DHPC lined pores and migration of DHPC away from those pores with increasing temperature.

AUTHOR INFORMATION

Corresponding Author

*E-mail: ayethiraj@mun.ca; mmorrow@mun.ca.

ACKNOWLEDGMENTS

This work was supported by the Natural Sciences and Engineering Research Council of Canada.

REFERENCES

(1) Sanders, C. R. II; Schwonek, J. P. *Biochemistry* **1992**, *31*, 8898−8905.
(2) Sanders, C. R. II; Hare, B. J.; Howard, K. P.; Prestegard, J. H. *Prog. NMR Spectrosc.* **1994**, *26*, 421−444.
(3) Sanders, C. R. II; Landis, G. C. *Biochemistry* **1995**, *34*, 4030−4040.
(4) Howard, K. P.; Opella, S. J. *J. Magn. Reson. B* **1996**, *112*, 91−94.
(5) Sanders, C. R.; Prosser, R. S. *Structure* **1998**, *6*, 1227−1234.
(6) Marcotte, I.; Auger, M. *Concepts Magn. Reson. Part A* **2005**, *24A*, 17−37.
(7) Sanders, C. R. In *Modern Magnetic Resonance*; Webb, G. A., Ed.; Springer: Netherlands, 2006; pp 233−239.
(8) Prosser, R. S.; Evanics, F.; Kitevski, J. L.; Al-Abdul-Wahid, M. S. *Biochemistry* **2006**, *45*, 8453−8465.
(9) Harroun, T. A.; Koslowsky, M.; Nieh, M.-P.; de Lanny, C.-F.; Raghunathan, V. A.; Katsaras, J. *Langmuir* **2005**, *21*, 5356−5361.
(10) Struppe, J.; Vold, R. R. *J. Magn. Reson.* **1998**, *135*, 541−546.
(11) Raffard, G.; Steinbruckner, S.; Arnold, A.; Davis, J. H.; Dufourc, E. J. *Langmuir* **2000**, *16*, 7655−7662.
(12) Sternin, E.; Nizza, D.; Gawrisch, K. *Langmuir* **2001**, *17*, 2610−2616.
(13) Triba, M. N.; Warschawski, D. E.; Devaux, P. F. *Biophys. J.* **2005**, *88*, 1887−1901.
(14) Gaemers, S.; Bax, A. *J. Am. Chem. Soc.* **2001**, *123*, 12343−12352.
(15) Soong, R.; Macdonald, P. M. *Biophys. J.* **2005**, *88*, 255−268.
(16) Kozak, M.; Kempka, M.; Szpotkowski, K.; Jurga, S. *J. Non-Cryst. Solids* **2007**, *353*, 4246−4251.
(17) Nieh, M.-P.; Glinka, C. J.; Kreuger, S.; Prosser, R. S.; Katsaras, J. *Biophys. J.* **2002**, *82*, 2487−2498.
(18) Gutberlet, T.; Hoell, A.; Kammel, M.; Frank, J.; Katsaras, J. *Appl. Phys. A: Mater. Sci. Process.* **2002**, *74*, S1260−S1261.
(19) Wang, H.; Nieh, M. P.; Hobbie, E. K.; Glinka, C. J.; Katsaras, J. *Phys. Rev. E* **2003**, *67*, 060902(R).
(20) Nieh, M.-P.; Raghunathan, V. A.; Glinka, C. J.; Harroun, T. A.; Pabst, G.; Katsaras, J. *Langmuir* **2004**, *20*, 7893−7897.
(21) Takajo, Y.; Matsuki, H.; Matsubara, H.; Tsuchiya, K.; Aratono, M.; Yamanaka, M. *Colloids Surf., B* **2010**, *76*, 571−576.
(22) Uddin, M. N.; Morrow, M. R. *Langmuir* **2010**, *26*, 12104−12111.
(23) Aussenac, F.; Laguerre, M.; Schmitter, J.-M.; Dufourc, E. J. *Langmuir* **2003**, *19*, 10468−10479.
(24) Rowe, B. A.; Neal, S. L. *Langmuir* **2003**, *19*, 2039−2048.
(25) van Dam, L.; Karlsson, G.; Edwards, K. *Biochim. Biophys. Acta* **2004**, *1664*, 241−256.
(26) Hwang, J. S.; Oweimreen, G. A. *Arabian J. Sci. Eng.* **2003**, *28*, 44−49.
(27) Vold, R. R.; Prosser, R. S.; Deese, A. J. *J. Biomol. NMR* **1997**, *9*, 329−335.

(28) Luchette, P. A.; Vetman, T. N.; Prosser, R. S.; Hancock, R. E. W.; Nieh, M.-P.; Glinka, C. J.; Krueger, S.; Katsaras, J. *Biochim. Biophys. Acta* **2001**, *1513*, 83−94.
(29) Andersson, A.; Mäler, L. *Langmuir* **2005**, *21*, 7702−7709.
(30) Andersson, A.; Mäler, L. *Langmuir* **2006**, *22*, 2447−2449.
(31) Nieh, M.-P.; Glinka, C. J.; Krueger, S.; Prosser, R. S.; Katsaras, J. *Langmuir* **2001**, *17*, 2629−2638.
(32) Katsaras, J.; Harroun, T. A.; Pencer, J.; Nieh, M.-P. *Naturwissenschaften* **2005**, *92*, 355−366.
(33) Nieh, M.-P.; Raghunathan, V. A.; Glinka, C. J.; Harroun, T.; Katsaras, J. *Macromol. Symp.* **2005**, *219*, 135−145.
(34) Nieh, M.-P.; Raghunathan, V. A.; Wang, H.; Katsaras, J. *Langmuir* **2003**, *19*, 6936−6941.
(35) Crowell, K. J.; Macdonald, P. *Biochim. Biophys. Acta* **1999**, *1416*, 21−30.
(36) Soong, R.; Macdonald, P. M. *Langmuir* **2009**, *25*, 380−390.
(37) Arnold, A.; Labrot, T.; Oda, R.; Dufourc, E. J. *Biophys. J.* **2002**, *83*, 2667−2680.
(38) Davis, J. H.; Jeffrey, K. R.; Bloom, M.; Valic, M.; Higgs, T. P. *Chem. Phys. Lett.* **1976**, *42*, 390−394.
(39) Prosser, R. S.; Davis, J. H.; Dahlquist, F. W.; Lindorfer, M. A. *Biochemistry* **1991**, *30*, 4687−4696.
(40) Davis, J. H. *Biochim. Biophys. Acta* **1983**, *737*, 117−171.
(41) Seelig, A.; Seelig, J. *Biochemistry* **1974**, *13*, 4839−4845.
(42) Lafleur, M.; Fine, B.; Sternin, E.; Cullis, P. R.; Bloom, M. *Biophys. J.* **1989**, *56*, 1037−1041.
(43) Cross, M. M. *J. Colloid Sci.* **1965**, *20*, 417−437.
(44) Förster, S.; Konrad, M.; Lindner, P. *Phys. Rev. Lett.* **2005**, 017803.
(45) Roux, D.; Nallet, F.; Diat, O. *Europhys. Lett.* **1993**, *24*, 53−58.
(46) Meyer, C.; Asnacios, S.; Bourgaux, C.; Kleman, M. *Rheol. Acta* **2000**, *39*, 223−233.
(47) Lu, C.-Y.; Chen, P.; Ishii, Y.; Komura, S.; Kato, T. *Eur. Phys. J. E* **2008**, *25*, 91−101.
(48) de Haas, K. H.; Blom, C.; van den Ende, D.; Duits, M. H. G.; Haveman, B.; Mellema, J. *Langmuir* **1997**, *13*, 6658−6668.
(49) Cates, M. E.; Candau, S. J. *J. Phys.: Condens. Matter* **1990**, *2*, 6869−6892.
(50) Cox, W. P.; Merz, E. H. *J. Polym. Sci.* **1958**, *28*, 619−622.
(51) Ianniruberto, G.; Marrucci, G. *J. Non-Newtonian Fluid Mech.* **1996**, *65*, 241−246.
(52) Sriram, I.; Furst, E. M.; DePuit, R. J.; Squires, T. M. *J. Rheol.* **2009**, *53*, 357−381.
(53) Bloom, M.; Sternin, E. *Biochemistry* **1987**, *26*, 2101−2105.
(54) Singh, H.; Emberley, J.; Morrow, M. R. *Eur. Biophys. J.* **2008**, *37*, 783−792.
(55) Russell-Schulz, B.; Booth, V.; Morrow, M. R. *Eur. Biophys. J.* **2009**, *38*, 613−624.
(56) Pauls, K. P.; MacKay, A. L.; Söderman, O.; Bloom, M.; Tangea, A. K.; Hodges, R. S. *Eur. Biophys. J.* **1985**, *12*, 1−11.
(57) Nieh, M.-P.; Raghunathan, V. A.; Pabst, G.; Harroun, T.; Nagashima, K.; Morales, H.; Katsaras, J.; Macdonald, P. *Langmuir* **2011**, *27*, 4838−4847.